In silico detection of inhibitor potential of *Passiflora* compounds against SARS-Cov-2(Covid-19) main protease by using molecular docking and dynamic analyses

Serap Yalçın [a,*], Seda Yalçınkaya [b], Fahriye Ercan [c]

[a] *Department of Molecular Biology and Genetics, Faculty of Art and Sciences, Kırsehir Ahi Evran University, Kırsehir 40100, Turkey*
[b] *Department of Food Engineering, Faculty of Engineering, Süleyman Demirel University, Isparta, Turkey*
[c] *Department of Plant Protection, Faculty of Agriculture, Kırşehir Ahi Evran University, Kırşehir, Turkey*

A B S T R A C T

SARS-Cov-2(Covid-19) is a new strain of coronavirus and was firstly emerged in December 2019 in Wuhan, China. Now, there is no known specific treatment of Covid-19 available. COVID-19 main protease is a potential drug target and is firstly crystallised by Liu et al (2020). In the study, we investigated the drug potential of molecules that the components of an important medicinal plant *Passiflora* by using molecular docking, molecular dynamic and drug possibility properties of these molecules. Docking performances were done by Autodock. Chloroquine, hydroxychloroquine were used as standarts for comparison of tested ligands. The molecular docking results showed that the Luteolin, Lucenin, Olealonic acid, Isoorientin, Isochaphoside, Saponarin, Schaftoside etc. ligands was bound with COVID-19 main protease above -8,0 kcal/mol binding energy. Besides, ADME, drug-likeness features of compounds of *Passiflora* were investigated using the rules of Lipinski, Veber, and Ghose. According to the results obtained, it has been shown that compounds of *Passiflora* have the potential to be an effective drug in the COVID-19 pandemic. Further studies are needed to reveal the drug potential of these ligands. Our results will be a source for these studies.

© 2021 Elsevier B.V. All rights reserved.

1. Introduction

Passiflora (passion flowers) is the largest genus of the family Passifloraceae. The species of this genus are distributed tropical regions of the World [1]. Many species of this genus have been found that contain anti-depressant properties. The leaves and the roots are generally more potent and have been used to improve the actions of mind-altering drugs. Few species of *Passiflora* have been studied according to its medicinal utility [2].

However, these plants have a major source of pharmacologically active compounds, including cytolysins, potential bactericid and anticancer drugs. For example, *Passiflora quadrangularis* is known with antihelminthic action and also often used to treat bronchitis, asthma, and whooping cough [3].

The new coronavirus type SARS-Cov 2 (severe acute respiratory syndrome), that appeared in December 2019 in China and became a global pandemic. There is not any specific treatment available so far. The viral particles effect both humans and animals, and can cause some serious infections of especially respiratory system. Besides, some drugs including chloroquine, remdesivir and hydroxychloroquine have been observed to be effective against Covid-19 [4].

Recent studies have shown that the genomic model of SARS-CoV 2 is comparable to other coronaviruses. It is stated that these viruses generally collect a few polypeptides in their life cycle and develop proteolytic degradation to produce 20 additional proteins. Among these proteases, it is emphasized that main protease (Mpro) and papain-like protease (PLpro) proteases are of vital importance in virus replication. Important studies have been done with these proteases to discover specific inhibitors against COVID-19. Yu et.al reported the calculation of the potential binding of luteolin and other natural components versus Mpro. It was concluded that luteolin also binds effectively with other target proteins of SARS-CoV-2 such as PLpro, Spike protein and RdRp [5].

An important therapeutic target for corona viruses is known to be the main protease, as this enzyme plays a key role in polyprotein processing and is active in a dimeric form [6]. Amin et al, 2021, stated that the main protease is the part of the replication machinery of the corona virus and can be used as a therapeutic
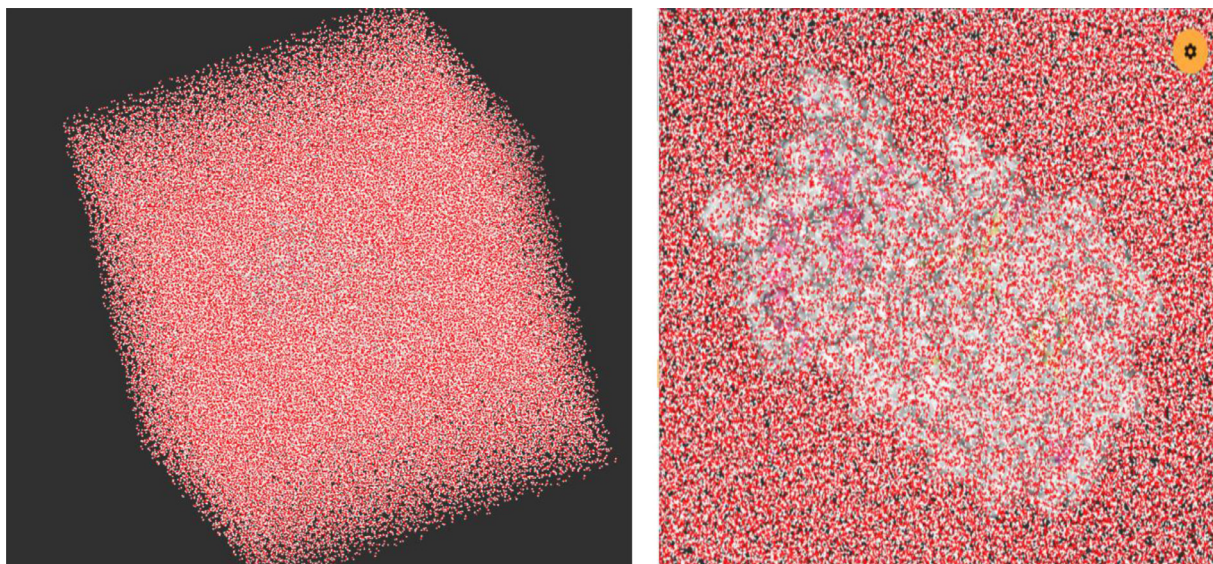

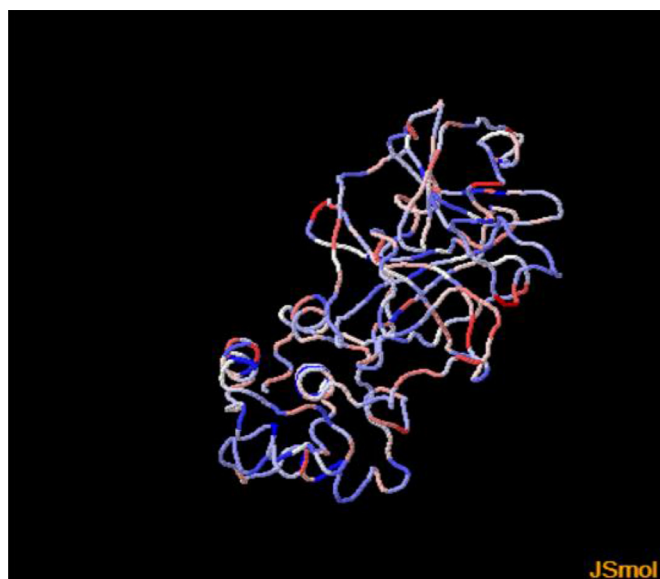Fig. 1. Solvation box of 6lu7(playmolecule.com).

Fig. 2. The energy distribution of protein [27,28].

target against the corona virus [7]. Li and Kang 2020, emphasized that the main protease encoded by the viral genome could be an attractive drug target, as it plays an important role in dividing viral polyproteins into functional proteins [8] In another study, it was noted that the sequence of the main protease is closely related to other betacoronaviruses and aids drug discovery studies based on previous lead compounds [9]. Ghosh et al., 2021, identified important molecular properties that regulate Mpro inhibitory properties [10]. All these studies reveal that the main protease is a suitable target for identifying potential drug substances. We also used the main protease in our study. Molecular docking is known a promising and useful tool for drug desing. In the present study, we investigated drug potential of *Passiflora* components against COVID-19 main (PDB ID: 6LU7). We aimed to find the most stable complex by revealing the binding energies.

Molecular docking is known a promising and useful tool for drug desing. In the present study, we investigated drug potential of *Passiflora* components against COVID-19 main (PDB ID: 6LU7). We aimed to find the most stable complex by revealing the binding energies.

2. Materials and methods

2.1. Molecular docking analyses

Molecular docking calculations were performed in Autodock Vina software [11]. The water molecules and cofactors were removed from the protein to clearly see the protein-ligand interation [12]. COVID-19 main protease used as a protein and the structure of this protein was freely available from the RCSB Protein Data Bank as a 3D theoretical model (PDB ID: 6LU7). Twenty nine ligands were tested. Ligands that used in the study and their properties were given in Table 1 (https://pubchem.ncbi.nlm.nih.gov/).

The binding potential of chloroquine and hydroxychloroquine has been reviewed as a control ligands. 2D structure of the ligands were converted to energy minimized 3D-structure. All protein and ligands were validated before performing the *in silico* computations [13].
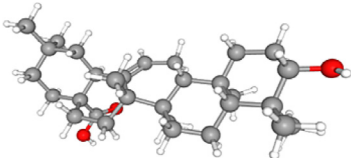
2.2. Molecular dynamic analyses
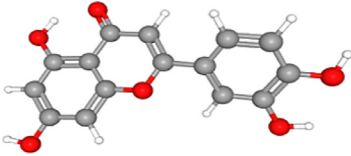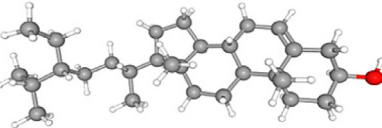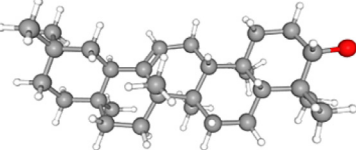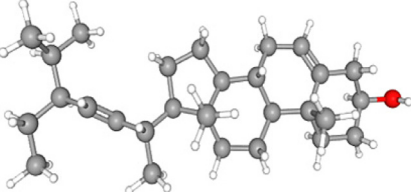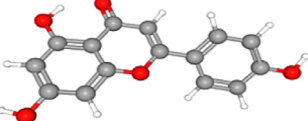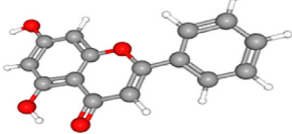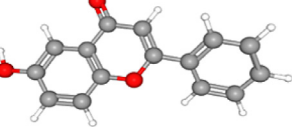
The simulation of the ligand-protein complex was performed using the playmolecule software [14–18] (**playmolecule.com**). MD simulation was performed for 20 ns to check the stability of the ligand-protein complexes [Fig. 1].

We determined the performance of MM/PB(GB)SA to identify the correct binding poses for ligands, including from the Schrödinger suite and Amber package (http://cadd.zju.edu.cn/farppi) [19].

2.3. Drug likeness and ADMET prediction for the components of Passiflora
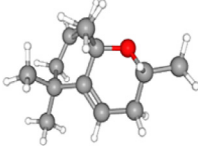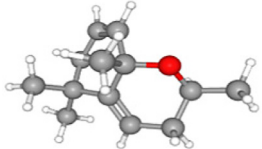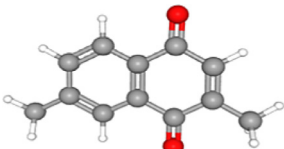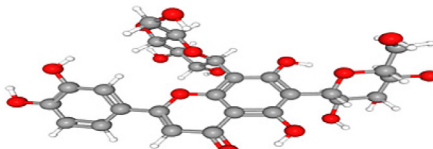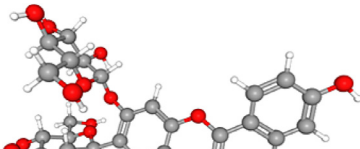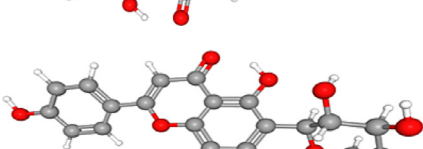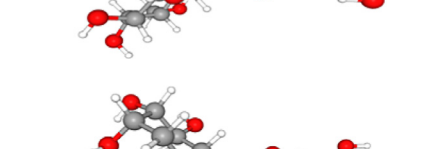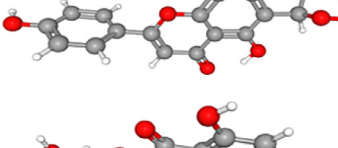
Currently, computer-based ADME analyses are gaining for drug discovery [20]. Pharmacokinetics and drug-likeness prediction of drug candidate molecule(s) was performed by online

Table 1
Ligands used in the study and their properties.

No	Ligands	PubChem ID code	Molecular weight(g.mol^{-1})	Structure(3D)
1	Oleanolic acid	10,494	456.7 g/mol	
2	Luteolin	5,280,445	286.24 g/mol	
3	Beta-Sitosterol	222,284	414.7 g/mol	
4	Beta-amyrin	73,145	426.7 g/mol	
5	Stigmasterol	5,280,794	412.7 g/mol	
6	Apigenin	5,280,443	270.24 g/mol	
7	Chrysin	5,281,607	254.24 g/mol	
8	6-Hydroxyflavone	72,279	238.24 g/mol	
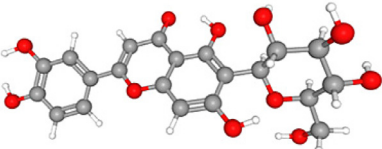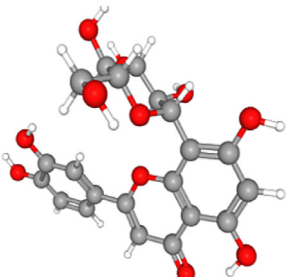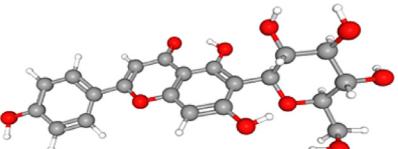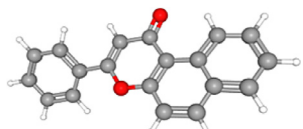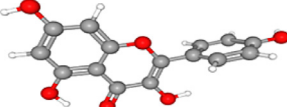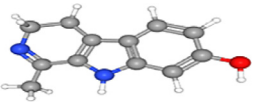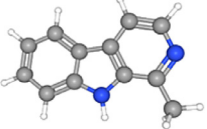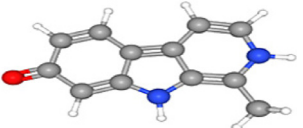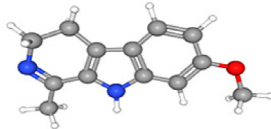
Table 1 (*continued*)

No	Ligands	PubChem ID code	Molecular weight(g.mol⁻¹)	Structure(3D)
9	Edulan-I	521,066	192.3 g/mol	
10	Edulan-II	6,432,428	192.3 g/mol	
12	Chimaphilin	101,211	186.21 g/mol	
13	Lucenin-2	442,615	610.5 g/mol	
14	Saponarin	441,381	594.5 g/mol	
15	Isoschaftoside	3,084,995	564.5 g/mol	
16	Schaftoside	442,658	564.5 g/mol	
17	Rutin	5,280,805	610.5 g/mol	

Table 1 (*continued*)

No	Ligands	PubChem ID code	Molecular weight(g.mol^{-1})	Structure(3D)
19	Isoorientin	114,776	448.4 g/mol	
20	Orientin	5,281,675	448.4 g/mol	
21	Isovitexin	162,350	432.4 g/mol	
21	5,6-benzoflavone	2361	272.3 g/mol	
22	Kaempferol	5,280,863	286.24 g/mol	
23	Harmalol	3565	200.24 g/mol	
24	Harman	5,281,404	182.22 g/mol	
25	Harmol	68,094	198.22 g/mol	
26	Harmaline	3564	214.26 g/mol	

Table 1 (*continued*)
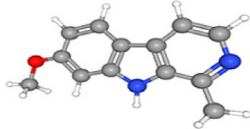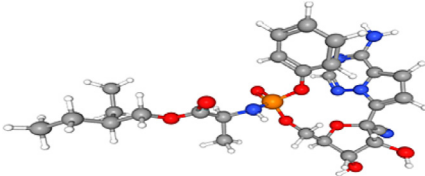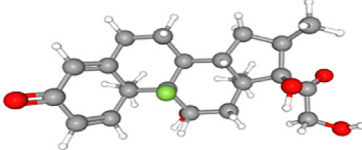
No	Ligands	PubChem ID code	Molecular weight(g.mol^{-1})	Structure(3D)
27	Harmine	5,280,953	212.25 g/mol	
28	Remdevisir	121,304,016	602.6 g/mol	
29	Dexamethasone	5743	392.5 g/mol	

Table 2
Target protein and drug candidate molecules (ligands) molecular docking results.

Ligands	Binding Energy (kcal/mol)	H bound
Oleanolic acid	-9.5 kcal/mol	1 Asp-A289
Luteolin	-8.3 kcal/mol	3 Gln-A110 Thr-A111 Asn-A151
Beta-Sitosterol	-8.0 kcal/mol	0
Beta-amylin	-8.0 kcal/mol	0
Stigmasterol	-7.6 kcal/mol	1 Arg-A105
Apigenin	-7.6 kcal/mol	1 Lys-A137
Chrysin	-7.3 kcal/mol	3 Asn-A238 Asp-A197 Lys-A137
6-Hydroxyflavone	-7.1 kcal/mol	1 Glu-A270
Edulan-I	-6.5 kcal/mol	1 Gln-A110
Edulan-II	-5.8 kcal/mol	0
Chimaphilin	-6.1 kcal/mol	2 Thr-A111 Gln-A110
Lucenin-2	-10.7 kcal/mol	4 Phe-A219 Leu-A220 Arg-A222 Asn-A274
Saponarin	-10.6 kcal/mol	3 Arg-A40(2) Phe-A181
Isoschaftoside	-10.5 kcal/mol	3 Arg-A222 Asn-274 Phe-A219

Table 2 (*continued*)

Ligands	Binding Energy (kcal/mol)	H bound
Schaftoside	-10.2 kcal/mol	5
		Asp-A197
		Asn-A238
		Arg-A131(2)
		Lys-A137
Rutin	-9.7 kcal/mol	5
		Arg-A131
		Lys-A137(2)
		Asp-A289(2)
Isoorientin	-9.2 kcal/mol	3
		Pro-A52
		Tyr-A54
		Phe-A181
Orientin	-8.7 kcal/mol	3
		Thr-A199
		Lys-A137
		Leu-A287
Isovitexin	-8.7 kcal/mol	3
		Glu-A55
		Pro-A52
		Tyr-A54
5,6-benzoflavone	-8.4 kcal/mol	1
		Gln-A110
Kaempferol	-7.5 kcal/mol	4
		Leu-A287
		Arg-A131
		Asp-A197
		Asn-A238
Harmalol	-6.0 kcal/mol	1
		Thr-A199
Harman	-5.8 kcal/mol	0
Harmol	-5.7 kcal/mol	0
Harmaline	-5.5 kcal/mol	0
Harmine	-5.4 kcal/mol	1
		Leu-A220
Remdesivir (Control)	-9.4 kcal/mol	1
		Lys-A137
	-8.0 kcal/mol	3
Dexamethasone (Control)		Lys-A137
		Thr-A198
		Tyr-A239

Table 3

Drug-likeness results of compounds.

Ligand	Drug likeness			Bioavalibility Score
	Lipinski	Ghose	Veber	
Oleanolic acid	Yes	No	Yes	0.56
	1 violation:	3 violations:		
	MLOGP>4.15	WLOGP>5.6, MR>130, #atoms>70		
Luteolin	Yes	Yes	Yes	0.55
Beta-Sitosterol	Yes	No	Yes	0.55
	1 violation:	3 violations:		
	MLOGP>4.15	WLOGP>5.6, MR>130, #atoms>70		
Beta-amyrin	Yes	No	Yes	0.55
	1 violation:	3 violations:		
	MLOGP>4.15	WLOGP>5.6, MR>130, #atoms>70		
Stigmasterol	Yes	No	Yes	0.55
	1 violation:	3 violations:		
	MLOGP>4.15	WLOGP>5.6, MR>130, #atoms>70		
Apigenin	Yes	Yes	Yes	0.55
Chrysin	Yes	Yes	Yes	0.55
6-Hydroxyflavone	Yes	Yes	Yes	0.55
Edulan-I	Yes	Yes	Yes	0.55
Edulan-II	Yes	Yes	Yes	0.55

Table 3 (*continued*)

Ligand	Drug likeness			Bioavalibility Score
	Lipinski	Ghose	Veber	
Chimaphilin	Yes	Yes	Yes	0.55
Lucenin-2	No; 3 violations: MW>500, NorO>10, NHorOH>5	No; 4 violations: MW>480, WLOGP<-0.4, MR>130, #atoms>70	No; 1 violation: TPSA>140	0.17
Saponarin	No; 3 violations: MW>500, NorO>10, NHorOH>5	No; 4 violations: MW>480, WLOGP<-0.4, MR>130, #atoms>70	No; 1 violation: TPSA>140	0.17
Isoschaftoside	No; 3 violations: MW>500, NorO>10, NHorOH>5			
	No; 3 violations: MW>480, WLOGP<-0.4, MR>130	No; 1 violation: TPSA>140	0.17	
Schaftoside	No; 3 violations: MW>500, NorO>10, NHorOH>5	No; 3 violations: MW>480, WLOGP<-0.4, MR>130	No; 1 violation: TPSA>140	0.17
Rutin	No; 3 violations: MW>500, NorO>10, NHorOH>5	No; 4 violations: MW>480, WLOGP<-0.4, MR>130, #atoms>70	No; 1 violation: TPSA>140	0.17
Isoorientin	No; 2 violations: NorO>10, NHorOH>5	No; 1 violation: WLOGP<-0.4	No; 1 violation: TPSA>140	0.17
Orientin	No; 2 violations: NorO>10, NHorOH>5	No; 1 violation: WLOGP<-0.4	No; 1 violation: TPSA>140	0.17
Isovitexin	Yes; 1 violation: NHorOH>5	Yes	No; 1 violation: TPSA>140	0.55
5,6-benzoflavone -	Yes	Yes	Yes	0.55
Kaempferol	Yes	Yes	Yes	0.55
Harmalol	Yes	Yes	Yes	0.55
Harman	Yes	Yes	Yes	0.55
Harmol	Yes	Yes	Yes	0.55
Harmaline	Yes	Yes	Yes	0.55
Harmine	Yes	Yes	Yes	0.55

Table 4
ADME results of compounds.

Ligands	Pharmacokinetics	
Oleanolic acid	GI absorption	Low
	BBB permeant	No
	P-gp substrate	No
	CYP1A2 inhibitor	No
	CYP2C19 inhibitor	No
	CYP2C9 inhibitor	No
	CYP2D6 inhibitor	No
	CYP3A4 inhibitor	No
	Log K_p (skin permeation)	-3.77 cm/s
Luteolin	GI absorption	High
	BBB permeant	No
	P-gp substrate	No
	CYP1A2 inhibitor	Yes
	CYP2C19 inhibitor	No
	CYP2C9 inhibitor	No
	CYP2D6 inhibitor	Yes
	CYP3A4 inhibitor	Yes
	Log K_p (skin permeation)	-6.25 cm/s
Beta-Sitosterol	GI absorption	Low
	BBB permeant	No
	P-gp substrate	No
	CYP1A2 inhibitor	No
	CYP2C19 inhibitor	No
	CYP2C9 inhibitor	No
	CYP2D6 inhibitor	No
	CYP3A4 inhibitor	No
	Log K_p (skin permeation)	-2.20 cm/s
Beta-amyrin	GI absorption	Low
	BBB permeant	No
	P-gp substrate	No

Table 4 (*continued*)

Ligands	Pharmacokinetics	
CYP1A2 inhibitor	No	
CYP2C19 inhibitor	No	
CYP2C9 inhibitor	No	
CYP2D6 inhibitor	No	
CYP3A4 inhibitor	No	
Log K_P (skin permeation)	-2.41 cm/s	
Stigmasterol	GI absorption	Low
BBB permeant	No	
P-gp substrate	No	
CYP1A2 inhibitor	No	
CYP2C19 inhibitor	No	
CYP2C9 inhibitor	Yes	
CYP2D6 inhibitor	No	
CYP3A4 inhibitor	No	
Log K_P (skin permeation)	-2.74 cm/s	
Apigenin	GI absorption	High
BBB permeant	No	
P-gp substrate	No	
CYP1A2 inhibitor	Yes	
CYP2C19 inhibitor	No	
CYP2C9 inhibitor	No	
CYP2D6 inhibitor	Yes	
CYP3A4 inhibitor	Yes	
Log K_P (skin permeation)	-5.80 cm/s	
Chrysin	GI absorption	High
BBB permeant	Yes	
P-gp substrate	No	
CYP1A2 inhibitor	Yes	
CYP2C19 inhibitor	No	
CYP2C9 inhibitor	No	
CYP2D6 inhibitor	Yes	
CYP3A4 inhibitor	Yes	
Log K_P (skin permeation)	-5.35 cm/s	
6-Hydroxyflavone	GI absorption	High
BBB permeant	Yes	
P-gp substrate	No	
CYP1A2 inhibitor	Yes	
CYP2C19 inhibitor	Yes	
CYP2C9 inhibitor	No	
CYP2D6 inhibitor	Yes	
CYP3A4 inhibitor	Yes	
Log K_P (skin permeation)	-5.18 cm/s	
Edulan-I	GI absorption	High
BBB permeant	Yes	
P-gp substrate	No	
CYP1A2 inhibitor	No	
CYP2C19 inhibitor	No	
CYP2C9 inhibitor	No	
CYP2D6 inhibitor	No	
CYP3A4 inhibitor	No	
Log K_P (skin permeation)	-5.36 cm/s	
Edulan-II	GI absorption	High
BBB permeant	Yes	
P-gp substrate	No	
CYP1A2 inhibitor	No	
CYP2C19 inhibitor	No	
CYP2C9 inhibitor	No	
CYP2D6 inhibitor	No	
CYP3A4 inhibitor	No	
Log K_P (skin permeation)	-5.36 cm/s	
Chimaphilin	GI absorption	High
BBB permeant	Yes	
P-gp substrate	No	
CYP1A2 inhibitor	Yes	
CYP2C19 inhibitor	Yes	
CYP2C9 inhibitor	No	
CYP2D6 inhibitor	No	
CYP3A4 inhibitor	No	
Log K_P (skin permeation)	-5.62 cm/s	
Lucenin-2	GI absorption	Low
BBB permeant	No	

Table 4 (*continued*)

Ligands	Pharmacokinetics	
P-gp substrate	No	
CYP1A2 inhibitor	No	
CYP2C19 inhibitor	No	
CYP2C9 inhibitor	No	
CYP2D6 inhibitor	No	
CYP3A4 inhibitor	No	
Log K_P (skin permeation)	-11.88 cm/s	
Saponarin	GI absorption	Low
BBB permeant	No	
P-gp substrate	Yes	
CYP1A2 inhibitor	No	
CYP2C19 inhibitor	No	
CYP2C9 inhibitor	No	
CYP2D6 inhibitor	No	
CYP3A4 inhibitor	No	
Log K_P (skin permeation)	-11.06 cm/s	
Isoschaftoside	GI absorption	Low
BBB permeant	No	
P-gp substrate	Yes	
CYP1A2 inhibitor	No	
CYP2C19 inhibitor	No	
CYP2C9 inhibitor	No	
CYP2D6 inhibitor	No	
CYP3A4 inhibitor	No	
Log K_P (skin permeation)	-11.30 cm/s	
Schaftoside	GI absorption	Low
BBB permeant	No	
P-gp substrate	Yes	
CYP1A2 inhibitor	No	
CYP2C19 inhibitor	No	
CYP2C9 inhibitor	No	
CYP2D6 inhibitor	No	
CYP3A4 inhibitor	No	
Log K_P (skin permeation)	-11.30 cm/s	
Rutin	GI absorption	Low
BBB permeant	No	
P-gp substrate	Yes	
CYP1A2 inhibitor	No	
CYP2C19 inhibitor	No	
CYP2C9 inhibitor	No	
CYP2D6 inhibitor	No	
CYP3A4 inhibitor	No	
Log K_P (skin permeation)	-10.26 cm/s	
Isoorientin	GI absorption	Low
BBB permeant	No	
P-gp substrate	No	
CYP1A2 inhibitor	No	
CYP2C19 inhibitor	No	
CYP2C9 inhibitor	No	
CYP2D6 inhibitor	No	
CYP3A4 inhibitor	No	
Log K_P (skin permeation)	-9.14 cm/s	
Orientin	GI absorption	Low
BBB permeant	No	
P-gp substrate	No	
CYP1A2 inhibitor	No	
CYP2C19 inhibitor	No	
CYP2C9 inhibitor	No	
CYP2D6 inhibitor	No	
CYP3A4 inhibitor	No	
Log K_P (skin permeation)	-9.14 cm/s	
Isovitexin	GI absorption	Low
BBB permeant	No	
P-gp substrate	No	
CYP1A2 inhibitor	No	
CYP2C19 inhibitor	No	
CYP2C9 inhibitor	No	
CYP2D6 inhibitor	No	
CYP3A4 inhibitor	No	
Log K_P (skin permeation)	-8.79 cm/s	
5,6-benzoflavone	GI absorption	High
BBB permeant	Yes	
P-gp substrate	No	
CYP1A2 inhibitor	Yes	
CYP2C19 inhibitor	Yes	
CYP2C9 inhibitor	No	
CYP2D6 inhibitor	No	

Table 4 (*continued*)

Ligands	Pharmacokinetics	
CYP3A4 inhibitor	No	
Log K_P (skin permeation)	-4.82 cm/s	
Kaempferol	GI absorption	High
BBB permeant	No	
P-gp substrate	No	
CYP1A2 inhibitor	Yes	
CYP2C19 inhibitor	No	
CYP2C9 inhibitor	No	
CYP2D6 inhibitor	Yes	
CYP3A4 inhibitor	Yes	
Log K_P (skin permeation)	-6.70 cm/s	
Harmalol	GI absorption	High
BBB permeant	Yes	
P-gp substrate	Yes	
CYP1A2 inhibitor	Yes	
CYP2C19 inhibitor	No	
CYP2C9 inhibitor	No	
CYP2D6 inhibitor	No	
CYP3A4 inhibitor	No	
Log K_P (skin permeation)	-6.28 cm/s	
Harman	GI absorption	High
BBB permeant	Yes	
P-gp substrate	Yes	
CYP1A2 inhibitor	Yes	
CYP2C19 inhibitor	No	
CYP2C9 inhibitor	No	
CYP2D6 inhibitor	No	
CYP3A4 inhibitor	Yes	
Log K_P (skin permeation)	-5.08 cm/s	
Harmol	GI absorption	High
BBB permeant	Yes	
P-gp substrate	No	
CYP1A2 inhibitor	Yes	
CYP2C19 inhibitor	No	
CYP2C9 inhibitor	No	
CYP2D6 inhibitor	No	
CYP3A4 inhibitor	Yes	
Log K_P (skin permeation)	-6.98 cm/s	
Harmaline	GI absorption	High
BBB permeant	Yes	
P-gp substrate	Yes	
CYP1A2 inhibitor	Yes	
CYP2C19 inhibitor	No	
CYP2C9 inhibitor	No	
CYP2D6 inhibitor	Yes	
CYP3A4 inhibitor	No	
Log K_P (skin permeation)	-6.14 cm/s	
Harmine	GI absorption	High
BBB permeant	Yes	
P-gp substrate	No	
CYP1A2 inhibitor	Yes	
CYP2C19 inhibitor	No	
CYP2C9 inhibitor	No	
CYP2D6 inhibitor	Yes	
CYP3A4 inhibitor	Yes	
Log K_P (skin permeation)	-4.94 cm/s	

tool SwissADME (http://www.sib.swiss) (http://www.swissadme.ch/index.php) [21,22]. In addition, these toxicological predictions have applied to Lipinski, Ghose, and Veber rules and bioavailability scores [23–25].

3. Results and discussion

Plant compounds have been always attractive from scientists to research novel drug development. The experimental and clinical studies are being continued for drug development, although several antiviral drugs used against Covid-19.

Molecular docking results obtained from this study indicated a strong interactions between COVID-19 main protease and potential drug candidates. The binding strength was defined by use of scoring function based on the Lamarckian Generic Algorithm. The binding free energy may include electrostatic, hydrogen bonding, and van der Waals interactions [12]. The least binding energy refers to the most stable binding between protein and the ligand

The binding energy results calculated by Vina were presented in Table 2 [Fig. 6]. All of the docked structures were visualized in VMD [26].

The Remdesivir and Dexamethasone which is control drugs, also binds to Covid-19 protein with considerable affinity (−9.4 and -8.0 kcal/mol, respectively). In this case, all the ligands have comparable binding affinity (−5.4 to −10.7 kcal/mol) (Figs. 2–4).

RSMD, a crucial parameter to analyze the equilibration of MD trajectories, is estimated for backbone atoms of the protein and ligand-protein complexes. Measurements of the backbone RMSD for the two complexes provided insights into the conformational stability. The comparisons of the RMSD value of ligands-protein are shown **in** Fig. 5.

The RMSF of the backbone atoms of each residue in the ligand-protein complex was analyzed to observe the flexibility of the enzyme backbone structure. The high RMSF value shows more flexibility whereas the low RMSF value shows limited movements. The RMSF graph for ligand**s**-protein complex is shown **in** Fig. 5**(a–g).**
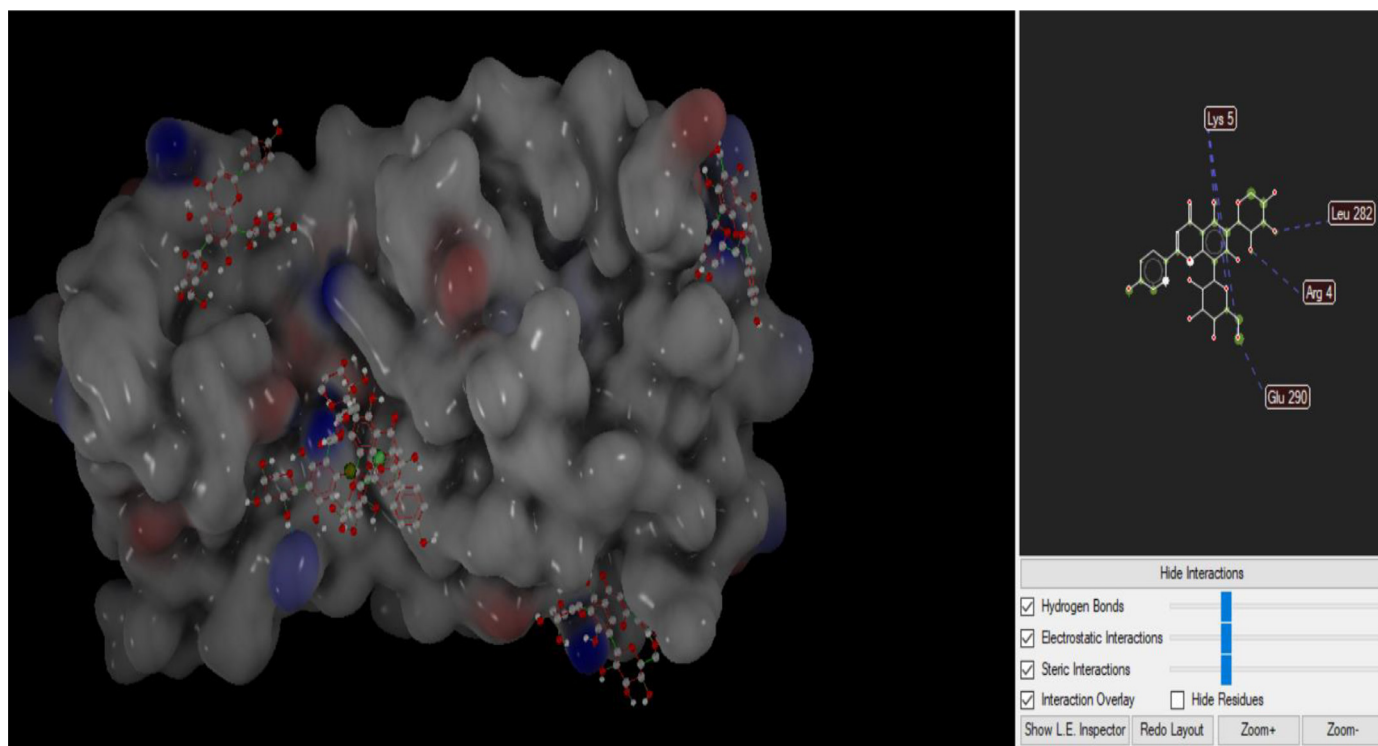
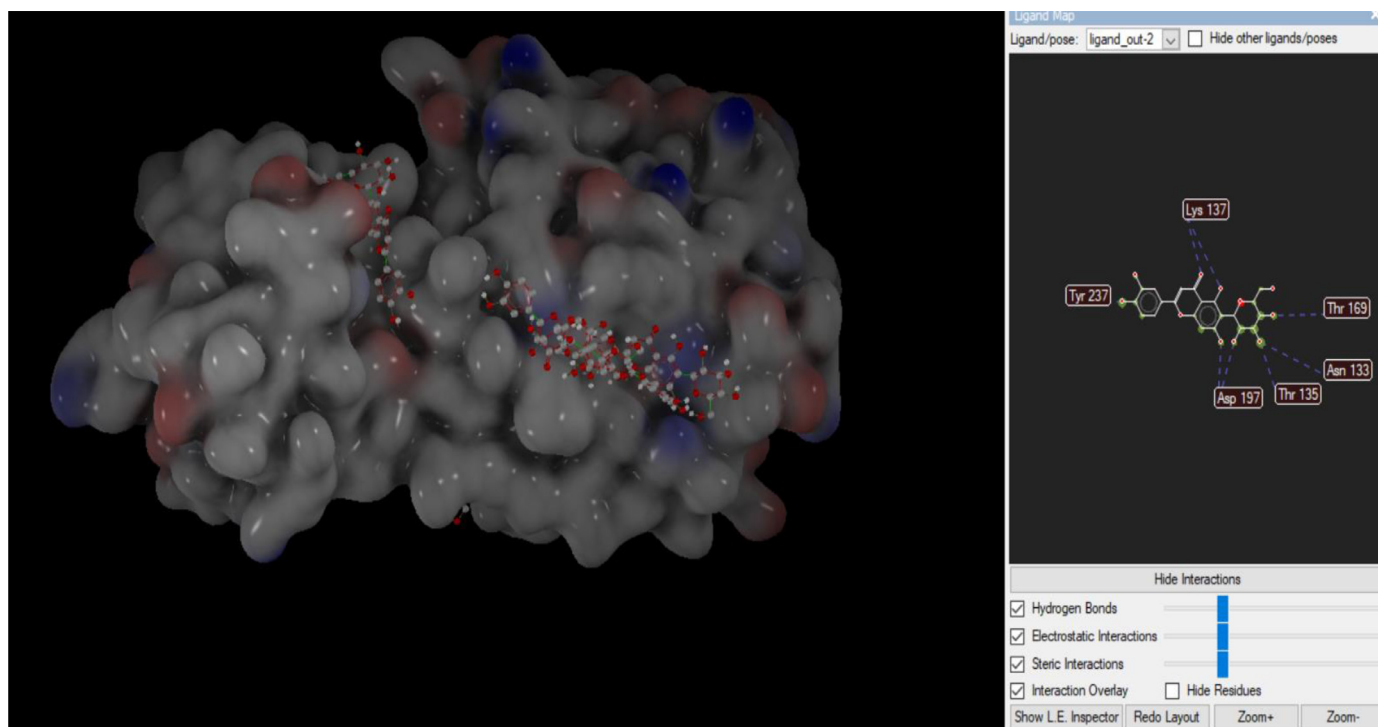**Fig. 3.** Representation of Isoschaftoside molecule at the active site of 6LU7 in molecular docking.

Fig. 4. Representation of Isoorientin molecule at the active site of 6LU7 in molecular docking.

According to molecular dynamic results, root mean square deviation (RMSD), root mean square fluctuation (RMSF) of Cα atoms as a function of residue number as a function of simulation time was used for studying the stability of the modeled domains during MD simulations. RMSD values of Isoorientin and Saponarin seem to be stable between 21 to 25 nanosecond.

Since molecular docking scoring did not indicate an acceptable prediction for ligand binding affinities, the MM/PB(GB)SA analyses were utilized to predict their binding affinities. MM/PB(GB)SA was determined to identify the binding free energy for ligands, including from the Schrödinger suite and Amber package (http://cadd.zju.
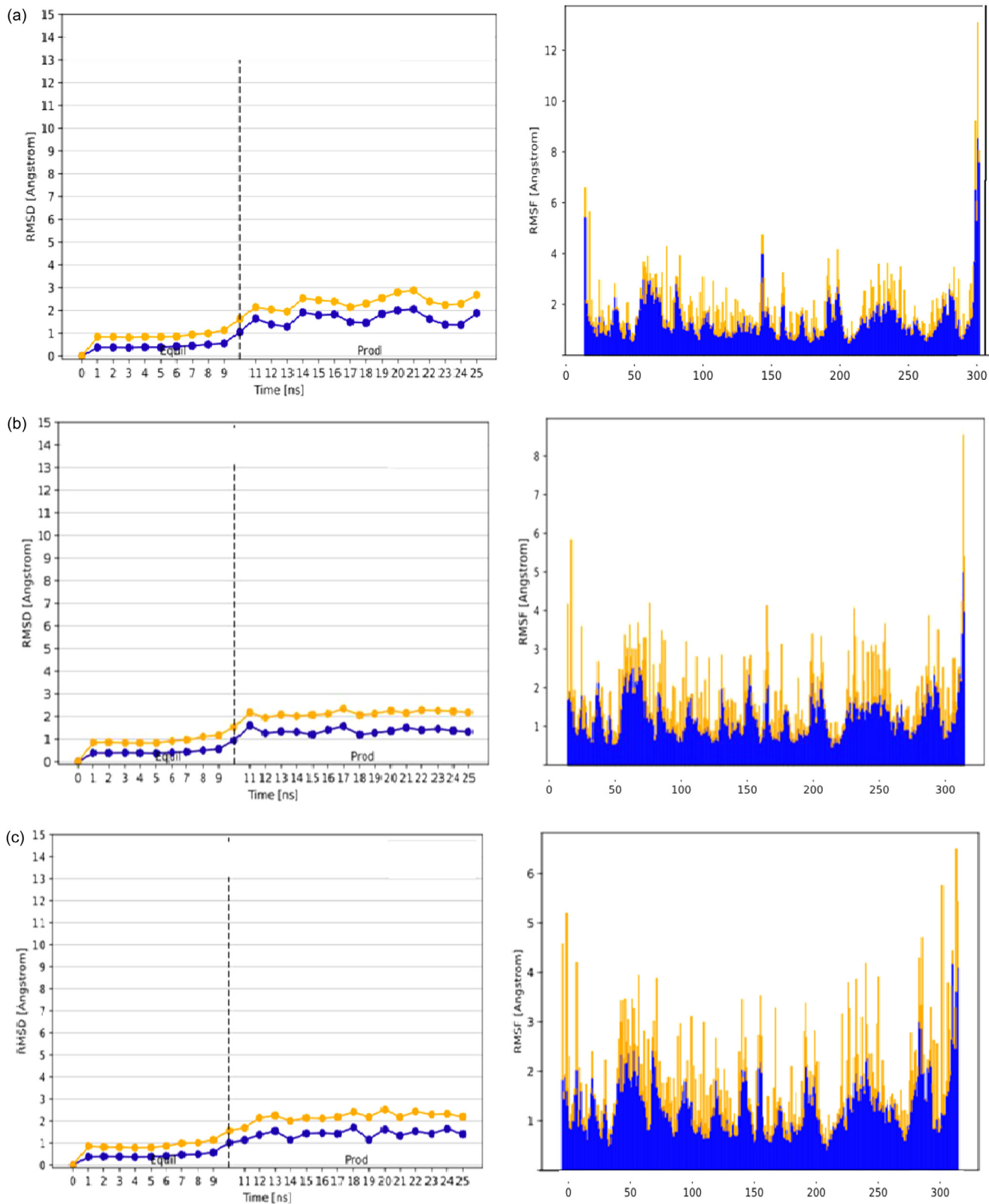
Fig. 5. (a) Lucenin2 and 6LU7 Molecular dynamic results. (b) Isoorientin and 6LU7 Molecular dynamic results. (c) Isoshaphoside and 6LU7 Molecular dynamic results. (d) Oleolanic acid and 6LU7 Molecular dynamic results. (e) Saponarin and 6LU7 Molecular dynamic results. (f) Schaftoside and 6LU7 Molecular dynamic results. (g) Molecular dynamic results of Remdevisir and 6lu7.
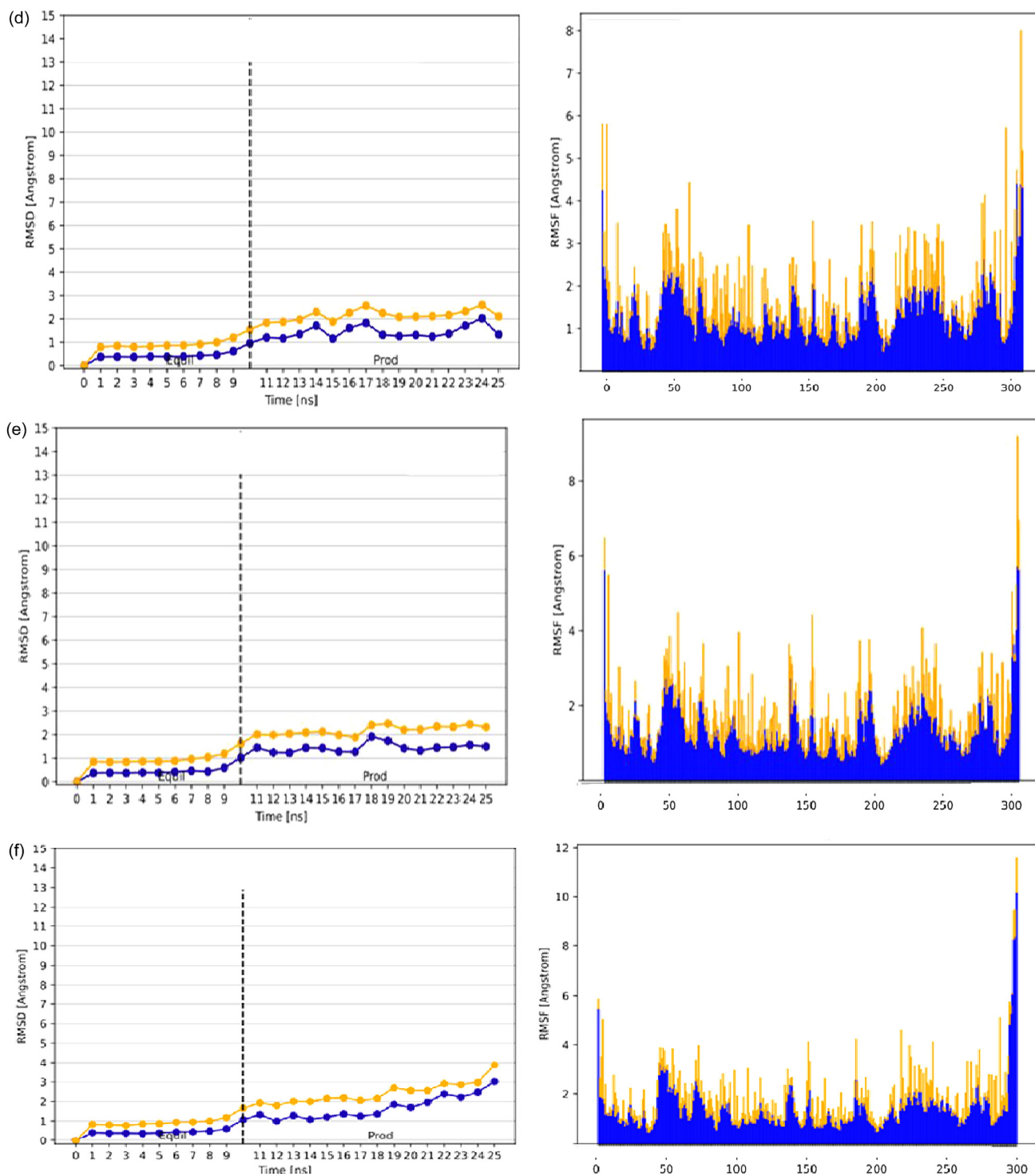
Fig. 5. Continued

edu.cn/farppi) **[19].** In Fig. 6(a–g) was shown MM/PB(GB)SA graph of ligands

Furthermore, human intestinal absorption, aqueous solubility levels, BBB penetration, skin penetretion levels, CYP inhibition (CYP1A2, CYP3A4, CYP2C19, CYP2C6, CYP2D6), P-gp subsrate of compounds of *Passiflora* were evaluated by prediction models in this study. (Supplementery file).

Drug-likeness can be characterized as a complex balance of different structural properties that determines whether a compound is a drug. These features, mainly lipophilicity, hydrogen bonding

properties, molecule size, and pharmacophoric features and many others **[29].** In addition, drug-likeness results of compounds were shown in Tables 3 and 4.

According to Lipinski's rule (Pfizer's rule, Lipinski's rule of five, RO5), the active drug has no more than one violation of the following properties including molecular weight(MW) $\leq$500, LogP $\leq$5, hydrogen bond acceptors $\leq$10, hydrogen bond donors $\leq$5 **[23]** .According to Veber rules, the active drug has total hydrogen bonds $\leq$ 12, rotatable bonds $\leq$ 10, and Polar surface area PSA (Polar surface area) $\leq$ 140 tend to have oral bioavailability $\geq$ 20% **[25]**. According
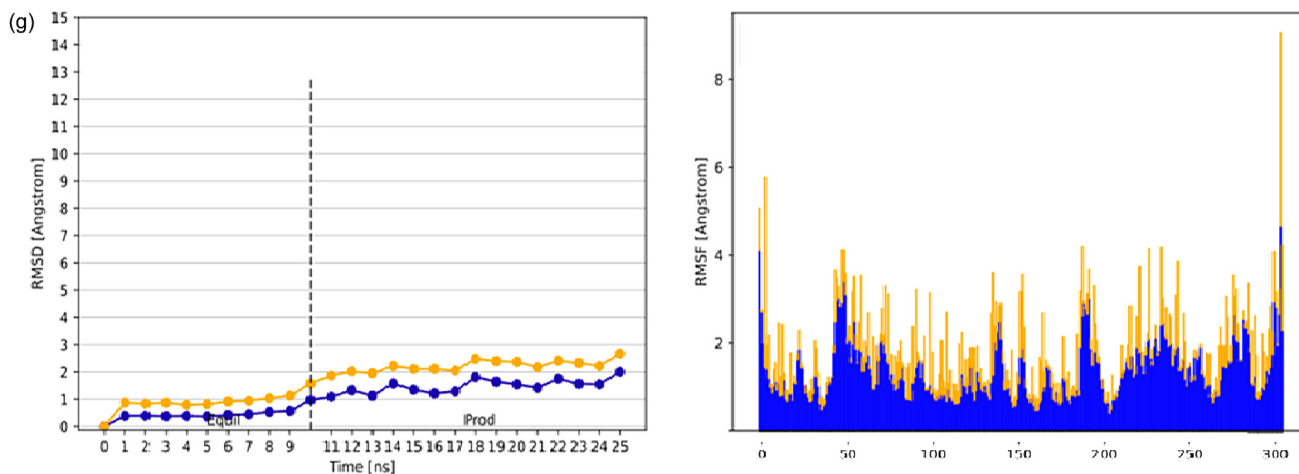
Fig. 5. Continued

to Ghose rules, active drug has Log P(-0.4 ~5.6), MR(Molar refractivity (40 ~150), MW(160 ~480), number of atoms(20 ~70), polar surface area (PSA) < 140 **[24]**.

Based on the drug-likeness analysis, Oleanolic acid, Luteolin, Beta-sitosterol, Beta-Amyrin, Sterigmasterol, Apigenin, Chrysin, 6-Hydroxyflavone, Edulan I and II, Chimaphilin, Isovixetin, 5,6,-benzoflavone, Kaempferol, Harmalol, Harman, Harmol, Harmaline, Harmine were found in accordance with the Lipinski's, Veber or Ghose' rule. However, Lipinski's rule of five may not apply to natural compounds. The only half of all FDA-approved small-molecule drugs are both used and compatible with the 'rule-of-five' **[30]**. Therefore, it has the potential to be used as a medicine in other molecules.

Today, drug development studies are based on irreversible inhibitors. Covalent inhibition is also a method used to obtain irreversible inhibition. Irreversible inhibitors interact with target proteins and the reaction tends to be complete rather than stable. Covalent inhibitors have some important advantages over non-covalent ones. Covalent inhibitors may act on target proteins by superficial binding cleavage leading to the development of new inhibitors with higher potency than non-covalent inhibitors. Covalent drugs generally have stronger binding affinity to the target due to the covalent bond between the ligand and the protein. Thus, they show stronger potential while maintaining the size of pharmacologically advantageous small molecules. Covalent interaction with

the target protein is an important point in terms of prolonging the duration of effect biologically. However, these inhibitors are a disadvantage as they tend to be toxic if they show off-target binding. Therefore, the presence of such inhibitors should be considered in drug development **[31]**.

4. Conclusion

Perforatum sp. used for many years as a medicinal plant for different treatments, has recently become popular with research for its different properties. This medicinal plant has become available since the beneficial effects it on human health. In our research based on this useful plant, the possibility of being used as a medicine in SARS-Cov-2 pandemic that our country and all countries of the world have been fighting for a long time has been investigated. Based on the results, it was concluded that *Perforatum* could be effective on SARS-Cov-2, but it is necessary to conduct laboratory tests *in vitro* and *in vivo* on animals and patients to approve their validity in inhibiting Covid-19.

Declaration of Competing Interest

The authors declare that they have no known competing financial interests or personal relationships that could have appeared to influence the work reported in this paper.
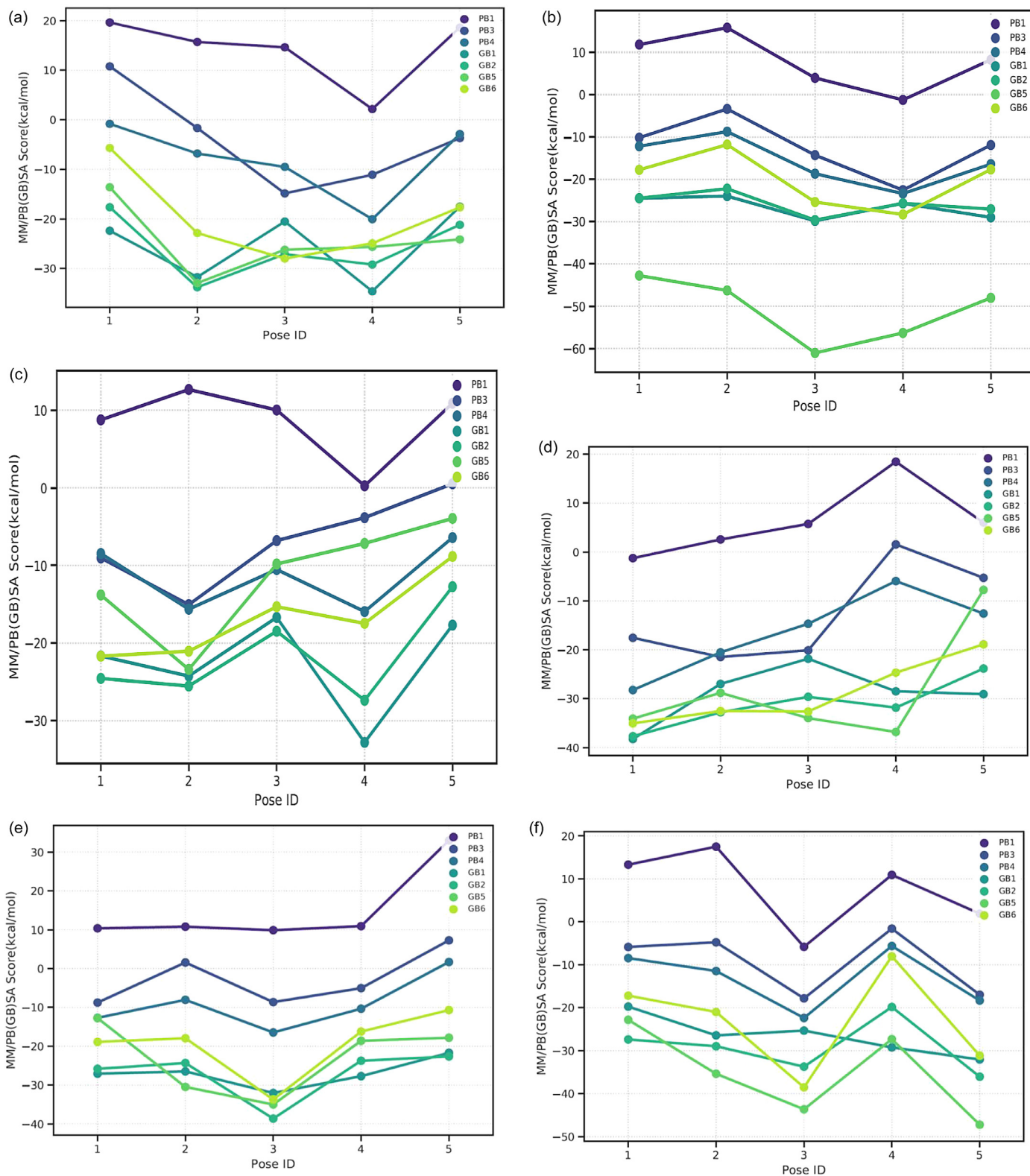
Fig. 6. (a) Binding free energy graph of Lucenin-2. (b) Binding free energy graph of Oleanolic acid. (c) Binding free energy graph of Isoorientin. (d) Binding free energy graph of Isoschaftoside. (e) Binding free energy graph of schaftoside. (f) Binding free energy graph of Saponarin. (g) Binding free energy graph of Remdivisir.
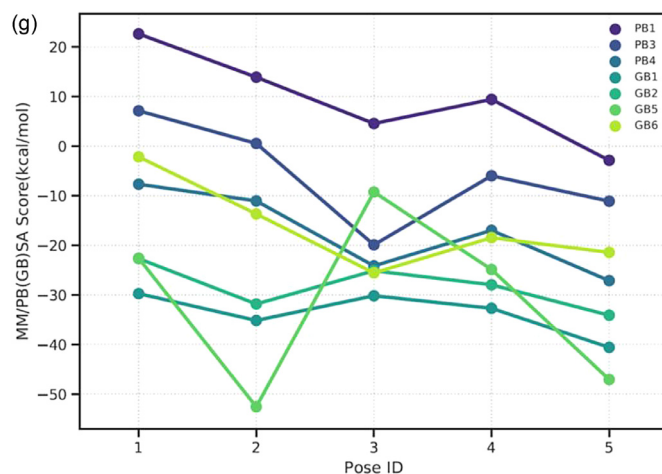
Fig. 6. Continued

References

[1] A.B. Montanher, S.M. Zucolotto, E.P. Schenkel, T.S. Fröde, Evidence of anti-inflammatory effects of *Passiflora* edulis in an inflammation model, J. Ethnopharmacol. 109 (2007) 281–288 https://doi.org/, doi:10.1016/j.jep.2006.07.031.

[2] S. Akhondzadeh, H.R. Naghavi, M. Vazirian, A. Shayeganpour, H. Rashidi, M. Khani, Passionflower in the treatment of generalized anxiety: a pilot double-blind randomized controlled trial with oxazepam, J. Clin. Pharm. Ther. 26 (2001) 363–367 https://doi.org/, doi:10.1046/j.1365-2710.2001.00367.x.

[3] D.B. Mowrey, in: Herbal Tonic Therapies, Wings Books, New York, 1993, p. p400.

[4] X. Liu, B. Zhang, Z. Jin, H. Yang, Z. Rao, The Crystal Structure of 2019-nCoV main Protease in Complex with an Inhibitor N3, RCSB Protein Data Bank, 2020 http://doi.10.2210/pdb6LU7/pdb.

[5] R Yu., L Chen, R Lan, R Shen, P Li., Computational screening of antagonists against the SARS-CoV-2 (COVID-19) coronavirus by molecular docking, Int. J. Antimicrob. Agents 56 (2020) 106012, doi:10.1016/j.ijantimicag.2020.106012.

[6] B. Goyal, D. Goyal, Targeting the dimerization of main protease of coronaviruses: a potential broad-spectrum therapeutic strategy, ACS Comb. Sci. (2020), doi:10.1021/acscombsci.0c00058.

[7] S. Abdul Amin, S. Banerjee, K. Ghosh, S. Gayen, T. Jha, Protease targeted COVID-19 drug discovery and its challenges: insight into viral main protease (Mpro) and papain-like protease (PLpro) inhibitors, Bioorg. Med. Chem. (2021) https://doi.org/, doi:10.1016/j.bmc.2020.115860.

[8] Q. Li, C. Kang, Progress in developing inhibitors of SARS-CoV-2 3C-like protease, Microorganisms 8 (2020) 1250, doi:10.3390/microorganisms8081250.

[9] S. Ullrich, C. Nitsche, The SARS-CoV-2 main protease as drug target, Bioorg. Med. Chem. Lett. 30 (2020) 127377 17, doi:10.1016/j.bmcl.2020.127377.

[10] K. Ghosh, S.A. Amin, S. Gayen, T. Jha, Chemical-informatics approach to COVID-19 drug discovery: exploration of important fragments and data mining based prediction of some hits from natural origins as main protease (Mpro) inhibitors, J. Mol. Struct. 1224 (2021) 129026, doi:10.1016/j.molstruc.2020.129026.

[11] O. Trott, A.J. Olson, AutoDock Vina: improving the speed and accuracy of docking with a new scoring function, efficient optimization, and multithreading, J. Comput. Chem. 31 (2010) 455–461, doi:10.1002/jcc.21334.

[12] E.B. Sas, S. Yalcin, F. Ercan, M. Kurt, A multi-spectroscopic, computational and molecular modeling studies on anti-apoptotic proteins with Boc-D-Lys-OH, J. Mol. Struct. 1199 (2020) 126981, doi:10.1016/j.molstruc.2019.126981.

[13] S. Yalcin, E.B. Sas, N. Cankaya, F. Ercan, M. Kurt, The physical studies and interaction with anti-apoptotic proteins of 2-(bis (cyanomethyl) amino)-2-oxoethyl methacrylate molecule, arXiv preprint arXiv:1910.00900 (2019) 10.5488/CMP.22.33301

[14] S. Doerr, M.J. Harvey, F. Noé, G. De Fabritiis, HTMD: high-throughput molecular dynamics for molecular discovery, J. Chem. Theory Comput. 12 (2016) 1845–1852 4https://doi.org/, doi:10.1021/acs.jctc.6b00049.

[15] R. Galvelis, Doerr S, J.M. Damas, M.J. Harvey, G. De Fabritiis, Parameterize: a fast molecular force field parameterization tool based on quantum-level machine learning, in preparation, J. Chem. Inf. Model. 26 (8) (2019) 3485–3493 59.

[16] J.S. Smith, B. Nebgen, N. Lubbers, O. Isayev, A.E. Roitberg, Less is more: sampling chemical space with active learning, J. Chem. Phys. 148 (2018) 241733 https://doi.org/, doi:10.1063/1.5023802.

[17] C. Devereux, J. Smith, K. Davis, K. Barros, R. Zubatyuk, O. Isayev, A. Roitberg, Extending the applicability of the ANI deep learning molecular potential to sulfur and halogens, J. Chem. Theory Comput. 16 (2020) 4192–4202 7, doi:10.1021/acs.jctc.0c00121.

[18] G. Martínez-Rosell, T. Giorgino, G. De Fabritiis, Playmolecule proteinprepare: a web application for protein preparation for molecular dynamics simulations, J. Chem. Inf. Model. 57 (2017) 1511–1516 7, 0.1021/acs.jcim.7b00190.

[19] Z. Wang, X. Wang, Y. Li, T. Lei, E. Wang, D. Li, Y. Kang, F. Zhu, T. Hou, farPPI: a webserver for accurate prediction of protein-ligand binding structures for small-molecule PPI inhibitors by MM/PB(GB)SA methods, Bioinformatics 35 (2019) 1777–1779, doi:10.1093/bioinformatics/bty879.

[20] F. Ntie-Kang, L.L. Lifongo, J.A. Mbah, L.C.O. Owono, E. Megnassan, L.M. Mbaze, S.M. Efange, *In silico* drug metabolism and pharmacokinetic profiles of natural products from medicinal plants in the Congo basin, Silico Pharmacol. 1 (2013) 12, doi:10.1186/2193-9616-1-12.

[21] V. Zoete, A. Daina, C. Bovigny, O. Michielin, SwissSimilarity: a web tool for low to ultra high throughput ligand-based virtual screening, J. Chem. Inf. Model. 56 (2016) 1399–1404, doi:10.1021/acs.jcim.6b00174.

[22] A. Daina, O. Michielin, V. Zoete, SwissADME: a free web tool to evaluate pharmacokinetics, drug-likeness and medicinal chemistry friendliness of small molecules, Sci. Rep. 7 (2017) 42717, doi:10.1038/srep42717.

[23] C.A. Lipinski, F. Lombardo, B.W. Dominy, P.J. Feeney, Experimental and computational approaches to estimate solubility and permeability in drug discovery and development settings, Adv. Drug Deliv. Rev. 23 (1997) 3–25, doi:10.1016/s0169-409x(00)00129-0.

[24] A.K. Ghose, V.N. Viswanadhan, J.J. Wendoloski, A knowledge-based approach in designing combinatorial or medicinal chemistry libraries for drug discovery. 1 A qualitative and quantitative characterization of known drug databases, J. Comb. Chem. 1 (1999) 55–68, doi:10.1021/cc9800071.

[25] D.F. Veber, S.R. Johnson, H.Y. Cheng, B.R. Smith, K.W. Ward, K.D. Kopple, Molecular properties that influence the oral bioavailability of drug candidates, J. Med. Chem. 45 (2002) 2615–2623, doi:10.1021/jm020017n.

[26] W. Humphrey, A. Dalke, K. Schulten, VMD-visual molecular dynamics, J. Mol. Gr. 14 (1996) 33–38, doi:10.1016/0263-7855(96)00018-5.

[27] M. Wiederstein, M.J. Sippl, ProSA-web: interactive web service for the recognition of errors in three-dimensional structures of proteins, Nucleic Acids Res. 35 (2007) W407–W410, doi:10.1093/nar/gkm290.

[28] M.J. Sippl, Recognition of errors in three-dimensional structures of proteins, Proteins 17 (1993) 355–362, doi:10.1002/prot.340170404.

[29] J.V. Turner, S. Agatonovic-Kustrin. In book: comprehensive medicinal chemistry II. (2007) . 10.1016/B0-08-045044-X/00147-4

[30] M.Q. Zhang, B. Wilkinson, Drug discovery beyond the 'rule-of-five, Curr. Opin. Biotechnol. 18 (2007) 478–488, doi:10.1016/j.copbio.2007.10.005.

[31] H.M. Kumalo, S. Bhakat, M.E.S. Soliman, Theory and applications of covalent docking in drug discovery: merits and pitfalls, Molecules 20 (2015) 1984–2000, doi:10.3390/molecules20021984.